Author Manuscript

Author Manuscript

Author Manuscript

Author Manuscript

HHS Public Access

Author manuscript

Neurosci Lett. Author manuscript; available in PMC 2019 June 21.

Published in final edited form as:

Neurosci Lett. 2018 June 21; 678: 55–61. doi:10.1016/j.neulet.2018.05.011.

Removal of area CA3 from hippocampal slices induces postsynaptic plasticity at Schaffer collateral synapses that normalizes CA1 pyramidal cell discharge

Theodore C. Dumas[1,2], **Michael R. Uttaro**[1], **Carolina Barriga**[1], **Tiffany Brinkley**[1], **Maryam Halavi**[1], **Susan N. Wright**[1], **Michele Ferrante**[1], **Rebekah C. Evans**[1], **Sarah L. Hawes**[1], and **Erin M. Sanders**[1]

[1]Krasnow Institute for Advanced Study, George Mason University, Fairfax, VA 22030

[2]Psychology Department, George Mason University, Fairfax, VA 22030

Abstract

Neural networks that undergo acute insults display remarkable reorganization. This injury related plasticity is thought to permit recovery of function in the face of damage that cannot be reversed. Previously, an increase in the transmission strength at Schaffer collateral to CA1 pyramidal cell synapses was observed after long-term activity reduction in organotypic hippocampal slices. Here we report that, following acute preparation of adult rat hippocampal slices and surgical removal of area CA3, input to area CA1 was reduced and Schaffer collateral synapses underwent functional strengthening. This increase in synaptic strength was limited to Schaffer collateral inputs (no alteration to temporoammonic synapses) and acted to normalize postsynaptic discharge, supporting a homeostatic or compensatory response. Short-term plasticity was not altered, but an increase in immunohistochemical labeling of GluA1 subunits was observed in the stratum radiatum (but not stratum moleculare), suggesting increased numbers of α-amino-3-hydroxy-5-methyl-4-isoxazolepropionic acid receptors and a postsynaptic locus of expression. Combined, these data support the idea that, in response to the reduction in presynaptic activity caused by removal of area CA3, Schaffer collateral synapses undergo a relatively rapid increase in functional efficacy likely supported by insertion of more AMPARs, which maintains postsynaptic excitability in CA1 pyramidal neurons. This novel fast compensatory plasticity exhibits properties that would allow it to maintain optimal network activity levels in the hippocampus, a brain structure lauded for its ongoing experience-dependent malleability.

Keywords

CA3 removal; fiber volley; field excitatory postsynaptic potential; hippocampus; homeostatic synaptic plasticity; population spike; Schaffer collateral; temporoammonic

Correspondence should be addressed to (include email address): Theodore C. Dumas, Ph.D., Associate Professor, Psychology Department, Krasnow Institute for Advanced Study, George Mason University, 4400 University Drive, MS 2A1, Fairfax, VA 22030, Phone: 703-993-9170, tdumas@gmu.edu.

Publisher's Disclaimer: This is a PDF file of an unedited manuscript that has been accepted for publication. As a service to our customers we are providing this early version of the manuscript. The manuscript will undergo copyediting, typesetting, and review of the resulting proof before it is published in its final citable form. Please note that during the production process errors may be discovered which could affect the content, and all legal disclaimers that apply to the journal pertain.

Author Manuscript Author Manuscript Author Manuscript Author Manuscript

Introduction

Neurons possess at least three distinct types of synaptic plasticity, 1) one that is directly responsive to patterned activity (primary activity-dependent plasticity), 2) a higher-order form that permits prior activity to influence plasticity induction at a future moment (metastatic plasticity), and 3) a regulatory form that maintains overall network activity in a working range (homeostatic plasticity). Trauma to the brain likely induce all three forms of synaptic plasticity as the system responds directly to the activity produced by the damage and attempts to regain stability (Rich and Wenner, 2007). Teasing apart the multiple types of plasticity that follow an acute injury is a challenge that may be met through electrophysiological recording in acutely prepares brain slices.

Homeostatic plasticity was first observed in neuronal cultures as a slow compensatory process in response to pharmacological adjustments in network activity levels (Turrigiano and Nelson, 2004). More specifically, following a few days of suppressed network activity, glutamatergic excitatory synapses displayed increased efficacy, due to global upward scaling of α-amino-3-hydroxy-5-methyl-4-isoxazolepropionic acid receptors (AMPARs) (Turrigiano et al., 1998; O'Brien et al., 1998; Ju et al., 2004; Sutton et al., 2006). Conversely, enhancement of network activity resulted in a global reduction in excitatory synaptic strength due to removal of AMPARs, demonstrating that homeostatic plasticity is bidirectional (Turrigiano et al., 1998; O'Brien et al., 1998). Homeostatic plasticity has also been reported in cultured tissue preparations (Aptowicz et al., 2004; Galvan et al., 2003; Royer and Pare, 2003; Dailey et al., 1994; Tyler and Pozzo-Miller, 2003; Kim and Tsien, 2008; Vlachos et al., 2012). In organotypic hippocampal cultures, application of TTX resulted in an increase in efficacy at mossy fiber and Schaffer collateral (SC-CA1) synapses and a concurrent reduction in synaptic strength at CA3-CA3 recurrent collaterals (Kim and Tsien, 2008). Thus, when homeostatic plasticity is induced in intact neuronal networks, multiple forms can be observed in the same neuron population (in this case, CA3 pyramidal neurons) under the same induction conditions.

In the vast majority of studies on homeostatic plasticity, activity of the network is pharmacologically altered, which leaves the tissue physically intact. Kim and Tsien (2008) surgically removed the dentate gyrus from organotypic hippocampal slice cultures on the day of preparation and later found a weakening of synaptic efficacy at CA3-CA3 recurrent collaterals (that shortened reverberatory bursts), indicating that homeostatic plasticity can be induced following removal of a specific excitatory input pathway. Likewise, removal of the entorhinal cortex from organotypic hippocampal slice cultures induces an increase in transmission efficacy at outer molecular layer synapses onto granule cells in the dentate gyrus (DG) (Vlachos et al., 2012). When area CA3 is removed from acutely prepared hippocampal slices, some of the Schaffer collateral axons die, but many survive and large population synaptic responses are retained in area CA1. This CA3-lacking preparation is routinely employed to increase the signal-to-noise ratio during intracellular recording from CA1 pyramidal cells by reducing the amount of spontaneous action potential-dependent transmitter release at SC-CA1 synapses (Mockett and Hulme, 2008). Given the findings of Kim and Tsien, (2008) and Vlachos et al (2012), it seems possible that CA3 removal may

Author Manuscript Author Manuscript Author Manuscript Author Manuscript

produce compensatory downstream physiological changes in area CA1. However, the typical incubation period of only two hours between slice preparation and recording would seem insufficient for the development of homeostatic plasticity. Interestingly, a fast form of homeostatic plasticity has been observed during blockade of action potentials in cortical (Ibata et al., 2008) and in hippocampal neuronal cultures (Sutton et al., 2006) and acutely prepared slices under conditions of neuronal silencing concurrent with blockade of spontaneous NMDA receptorresponses (Félix-Oliveira et al., 2014), warranting further exploration of possible fast homeostatic plasticityat SC-CA1synapses after removal of area CA3.

To investigate the potential for synaptic plasticity following CA3 resection, we prepared hippocampal slices and immediately removed area CA3 from half of them. At two or more hours after slice preparation, population field responses recorded in stratum radiatum of area CA1 revealed a reduction in the number of functional Schaffer collateral input fibers to CA1 pyramidal neurons (SC-CA1) and an increase in SC-CA1 synaptic strength in the slices with area CA3 removed. The population spike recorded in the stratum pyramidale was not different between slice groups, supporting the possibility that the increase in SC-CA1 synaptic efficacy as homeostatic, normalizing excitability in CA1 pyramidal cells. Short-term plasticity was not altered, suggesting no change in transmitter release properties and temporoammonic to CA1 pyramidal cell (TA-CA1) synapses responses were unaffected, suggesting synapse-specificity. Removal of area CA3 increased the immunohistochemical labeling of AMPAR subunits in the stratum radiatum, but not stratum moleculare, supporting a postsynaptic site of expression limited to the manipulated input pathway. These data reveal a novel form of plasticity that may be rapid enough to maintain hippocampal network activity in an optimal working range amidst constant and substantial activity-dependent plasticity.

Materials and Methods

Subjects

Male Long Evans rats bred in the Krasnow Institute Animal Facility served as subjects for this study. Original and replacement breeders were purchased from Charles River Labs (Frederick, MD). Animals were maintained on a 12:12 hour light dark cycle with lights coming on at 7 am. Water and food were available ad libitum. All procedures were performed in accordance with the regulations stated in the *Guide for Care and Use of Laboratory Animals* by the National Research Council and approved by the George Mason University Institutional Animal Care and Use Committee.

Electrophysiological Recording

We prepared hippocampal slices from adult (3–6 months old) rats. Animals were deeply anesthetized with Isoflurane and decapitated. Brain dissection and slicing (450 μm thick transverse slices) were performed in ice-chilled, oxygenated (95% O_2, 5% CO_2) artificial cerebrospinal fluid (ACSF in mM: NaCl 124, KCl 2, $MgSO_4$ 2, $CaCl_2$ 2, KH_2PO_4 1.25, $NaHCO_3$ 26, and glucose 10, pH 7.4). Slices were immediately transferred to an interface chamber (Harvard Apparatus, Holliston, MA) and perfused with oxygenated ACSF (1.5 ml/

Author Manuscript Author Manuscript Author Manuscript Author Manuscript

min) at room temperature. Once placed in the recording chamber, a sterile razor blade was used to remove area CA3 from half of the slices (Fig. 1) counterbalanced for position within the chamber. Recording commenced no earlier than two hours after slice preparation. A bipolar platinum iridium stimulating electrode was positioned in the stratum radiatum of area CA1 to induce field potentials that were recorded by separate glass electrodes (1–8 MΩ, filled with ACSF) placed in the stratum radiatum and stratum pyramidale. Stimulation pulses (monophasic, 100 μs) of varying intensity (10, 25, 50, 100, 200, 400 μA, 5 sweeps per level) were delivered to create input-output (I/O) curves. To address presynaptic function, stimulation intensity was set to evoke a baseline synaptic field response of 1 mV (roughly 25–30% of the average maximum amplitude) and then pairs of stimulation pulses were applied with an inter-stimulus intervals (ISIs) of 25, 50, 100, 200 ms (5 sweeps per ISI). Following recording of I/O and ISI curves, thirty-pulse bursts were delivered at 5, 20, and then 40 Hz. Five minute intervals were imposed between bursts and the fEPSP slope returned to baseline.

In separate slices, the stimulating electrode was moved toward the hippocampal fissure on the subiculum side of the recording electrode to activate temporoammonic to CA1 pyramidal cell TA-CA1 synapses (Fig. 1) and I/O curves were recorded as performed for SC-CA1 inputs.

Immunohistochemistry

Slices were prepared the same as for electrophysiological recording. At two hours after incubation, the slices were transferred to paraformaldehyde (PFA, 4% in phosphate-buffered saline, PBS) for 15–30 minutes and then embedded in gelatin in 1.5 mL plastic centrifuge tubes. Tubes were left open overnight to set the gelatin and then a razor blade was used to cut a cylinder from the tube containing the slice. The gelatin disk containing the slice was post-fixed in 4% PFA overnight at 4°C and then transferred to PBS. Each gelatin disk was sectioned in a vibratome (30 μm thickness) and sections were stored in PBS at 4°C.

Prior to labeling, sections were incubated in blocking solution (5% normal goat serum and 0.3% Triton X-100 in PBS) on rocker plate at room temperature for one hour and then washed three times in PBS (15 minutes per wash at room temperature). Washed sections were incubated in anti-GluA1 primary antibody (1:200 dilution in blocking solution, Millipore Cat# AB1504 RRID:AB_2113602) for 72 hours rocking at 4°C. Labeled sections were washed three times in PBS for (15 minutes per wash at room temperature) and incubated in anti-rabbit secondary antibody conjugated to Cy3 (1:500 dilution, Millipore Cat# AP132C RRID:AB_92489) for 4 hours rocking at room temperature. Sections were washed (15 minutes per wash at room temperature) and mounted on microscope slides with fluorescent mounting medium (Vector Labs, Vectashield) for viewing on an epifluorescence microscope (Olympus, BX51wi). Microscope illumination intensity and detector sensitivity were determined in slices that were treated with secondary, but not primary antibody, and then applied to all sections within each experiment.

Author Manuscript Author Manuscript Author Manuscript Author Manuscript

Data Analyses

The FV amplitude was taken as the voltage value between two cursors, one placed at the response onset and the other at its most negative deflection (Clampfit, pClamp, Molecular Devices). The fEPSP slope was calculated within a 0.8 ms window at the initial descending phase of the response. The PS amplitude was calculated as the voltage difference between two cursors, one at the leading positive peak and one at the most negative peak of the response. Cursor placements for parameter extraction are shown in Figure 1.

For measurement of the immunohistochemical GluA1 signal intensity, extraction regions were drawn in the stratum radiatum and stratum moleculare of area CA1 to approximate the recording sites and also in the stratum moleculare of the dentate gyrus (Figs. 1, 5). The stratum radiatum region of interest was localized similarly across slices with respect to distance from the stratum pyramidale and distance from the knife cut. The extraction region for stratum moleculare in area CA1 was always immediately juxtaposed (above) to the fissure and spanned the entire layer. For the stratum moleculare in the DG, the extraction region was centered in the dendritic region of the superior blade just below the extraction box for stratum moleculare in area CA1. To place the extraction regions consistently on the CA3+ images, a line was drawn to represent the knife cut. Average intensity within each region was calculated by Metamorph software. Intensity values from three sections per slice (one slice per animal) were averaged. Average intensity values for area CA1 strata radiatum and moleculare were normalized by the intensities recorded in the dentate gyrus, a region upstream from the CA3 removal. Values used for statistical comparisons are averages of raw signal intensity values 2–4 sections per animal.

Two-way repeated-measures ANOVAs were applied to compare across slice groups and stimulation intensity (for I/O curves), ISI (for ISI curves), or pulse number (for 30-pulse bursts). Since no data sets passed Mauchly's test for sphericity, the Greenhouse-Geisser correction was applied. An unpaired t-test was employed to compare normalized GluA1 labeling intensity across slice conditions in the strata radiatum and moleculare. All figures display the group means and error bars are standard error of the mean.

Results

We first recorded the field potentials resulting from Schaffer collateral activation at varying the stimulation intensity to create I/O curves. The fiber volley (FV) amplitude, a measure of the number of afferents being activated, increased across stimulation intensities for both groups (two-way repeated-measures ANOVA: main effect of stimulation intensity, [$F(1.1, 34.3) = 139.87$, $p < 0.0001$] (Fig. 2A). However, the FV was reduced in slices that underwent CA3 removal [main effect of slice preparation, $F(1, 31) = 5.58$, $p < 0.03$]. There was also an interaction between the slice preparation (CA3+, CA3-) and stimulus intensity reflective of the increased group differences with increasing stimulation intensity [$F(1.1, 34.3) = 4.94$, $p < 0.05$].

SC-CA1 synapses provide the bulk of synaptic excitation to CA1 pyramidal neurons. Comparison of field excitatory postsynaptic potential (fEPSP) slopes upon activation of SC-CA1 synapses revealed a main effect of stimulation intensity [two-way repeated-measures

Author Manuscript Author Manuscript Author Manuscript Author Manuscript

ANOVA: F(1.3, 40.3) = 4.94, p < 0.0001] but no effect of CA3 removal and no interaction (Fig. 2B). Since a reduction in the FV was not accompanied by a reduction in the fEPSP, we divided the fEPSP slope by the FV amplitude to produce fEPSP to FV ratio (fEPSP/FV) values. The mean fEPSP/FV varied across stimulation intensity [two-way repeated-measures ANOVA: main effect of stimulation intensity, F(2.4, 73.2) = 4.94, p < 0.02] and the fEPSP/FV values were consistently larger for slices that underwent CA3 removal compared to intact slices [main effect of slice preparation, F(1, 31) = 5.05, p < 0.05], indicating an increase in synaptic strength at CA3-CA1 synapses (Fig. 2C).

A sufficiently intense activation pulse applied to Schaffer collaterals produces a supra-threshold fEPSP and a compound action potential (population spike, PS) that can be recorded in the CA1 cell body layer. Recordings made in the cell body layer revealed an increase in the PS amplitude with increasing stimulation intensity [two-way repeated measures ANOVA: main effect of stimulation intensity, F(1.2, 12.7) = 14.34; p < 0.002], but there was no effect of CA3 removal (Fig. 2D). Combined with the effects on synaptic transmission recorded in stratum radiatum, it appears that the increase in efficacy at SC-CA1 synapses compensates for the reduction in Schaffer collateral input following CA3 resection and maintains postsynaptic discharge in CA1 pyramidal cells. Figure 2E shows the direct input-output relationship by plotting the PS against the FV. It is clear that the reduced input into CA1 after CA3 removal is able to drive the same level of postsynaptic excitation. However, the FV reflects a response to electrical stimulation and is not a measure of on-going spontaneous activity. Thus, while the output from CA1 is normalized, it is still necessary to show that the spontaneous activity at Schaffer collateral axons is reduced to more accurately define the synaptic plasticity as homeostatic.

Paired-pulse facilitation (PPF) of the fEPSP slope was calculated. To test for a presynaptic locus for the increase in synaptic strength, we first delivered pairs of stimulation pulses at varying ISIs and analyzed the resultant PPF of the fEPSP. While PPF magnitude varied across ISIs [two-way repeated measures ANOVA: main effect of ISI, F(2.8, 105.3) = 4.08; p < 0.01], there was no effect of CA3 removal, suggesting that the increase in synaptic strength associated with CA3 removal was not a function of increased transmitter release probability (Fig. 3A). We followed up by applying 30-pulse bursts at 5, 20, or 40 Hz. In all cases, the normalize fEPSP slope was modified across the burst [two-way repeated measures ANOVA: main effect of pulse number, 5 Hz: F(3.8, 48.8) = 7.34; p < 0.0001; 20 Hz: F(2.9, 40.4) = 37.4; p < 0.0001; 40 Hz: F(4.3, 114.8) = 219.10; p < 0.0001], but there were no differences across slice preparations (Fig. 3B, 3C, 3D) further supporting no modification in presynaptic function due to CA3 removal.

To determine whether these homeostatic synaptic modifications were global (cell autonomous) or specific to the fibers that had been cut, we recorded evoked TA-CA1 synaptic responses. The FV amplitude (Fig. 4A) and fEPSP slope (Fig. 4B) both increased across stimulation levels [two-way repeated measures ANOVA: main effect of stimulation intensity, FV: F(1.5, 61.8) = 197.61; p < 0.0001; fEPSP: F(1.8, 72.8) = 213.00; p < 0.0001], but there were no differences across slice groups. Mean fEPSP/FV values were altered by varying stimulation intensity [main effect of stimulation intensity, F(2.4, 95.4) = 9.72; p <

Author Manuscript Author Manuscript Author Manuscript Author Manuscript

0.0001], but not by CA3 removal (Fig. 4C). These data support no alterations at TA-CA1 synapses and an effect of CA3 removal that is specific to SC-CA1 synapses.

To test for alterations in postsynaptic receptors as a factor underlying the increase in synaptic strength produced by CA3 removal, we performed immunohistochemistry for glutamate receptor subunits in hippocampal slices that were prepared by the same methods used for electrophysiological recording. After fixation and sectioning, sections were incubated in antibodies targeting GluA1 followed by incubation in a fluorescent secondary antibody. Signal intensities from the strata radiatum and moleculare in area CA1 (Fig. 5A) were normalized by the mean intensity measure in the molecular layer of the superior blade of the dentate gyrus, an upstream excitatory synaptic population. No difference was observed in average raw signal intensity in the dentate gyrus between slice conditions [$t(13) = 1.35$, $p = 0.10$] (Fig. 5B). The average normalized signal intensity for GluA1 in the stratum radiatum, the primary locus for Schaffer-collateral innervation of CA1 pyramidal neurons, was increased in slices that underwent CA3 removal compared to intact slices [$t(13) = 1.81$; $p = 0.04$). In the stratum moleculare, which contains afferents arriving at CA1 directly from the entorhinal cortex, the normalized GluA1 signal intensity was not affected by slice preparation [$t(13) = 0.79$, $p = 0.22$]. Combined, the results suggest a synapse-specific up-regulation of GluA1 expression at SC-CA1 synapses following CA3 removal and support the idea that the homeostatic increase in synaptic strength is supported by an increase in the number of postsynaptic AMPARs. Lack of a change in the GluA1 signal in the stratum moleculare and visible differences between the DG and area CA1 argue against non-specific antibody labeling and supports a synapse-specific alteration in AMPARs. Verification of these immunohistochemical experiments with additional antibodies, spine markers, and higher resolution microscopy is warranted.

Discussion

Synopsis

This report describes a fast-acting, synapse-specific form of synaptic plasticity that appears to be homeostatic. Specifically, in acutely prepared hippocampal slices from young adult rats, we showed that homeostatic plasticity at SC-CA1 synapses occurs by two hours after removal of area CA3. A substantial component of the functional input from area CA3 remained intact as evidenced by large FVs in both groups. However, there was a significant reduction in the FV magnitude after CA3 removal. In response, SC-CA1 synapses displayed an increase in efficacy, which acted to maintain the magnitude of synaptically-elicited postsynaptic discharge in CA1 pyramidal cells. The increase in synaptic strength was not associated with any changes in presynaptic function, but was associated with an increase in GluA1 labeling in the stratum radiatum immediately downstream from the CA3 resection, but not in the stratum moleculare, signifying a postsynaptic site of expression and indicating some degree of synapse specificity. There was no effect of CA3 removal on the efficacy of TA synapses, further supporting synapse specificity. However, an effect of CA3 removal at TA-CA1 synapses may have been occluded by homeostatic plasticity induced by removal of the entorhinal cortex (Vlachos et al., 2012). Thus, we have shown that a common practice of removing area CA3 from hippocampal slices to increase the signal to noise ratio during

Author Manuscript Author Manuscript Author Manuscript Author Manuscript

intracellular recordings from CA1 pyramidal neurons induces upscaling of excitatory SC-CA1 synaptic transmission that normalizes postsynaptic excitability. To define this response to acute injury as fast homeostatic synaptic plasticity, it will be necessary to record during the recovery period to determine if there is a reduction in spontaneous input activity and to determine more precisely when the synaptic strengthening occurs. To further define the plasticity response to CA3 removal, more accurate FV amplitude measurements may be made during blockade of the synaptic response (application of AMPA and NMDA receptor blockers), more specific synaptic alterations may be identified by recording whole-cell currents from individual CA1 pyramidal neurons, and the CA3 removal can be replicated under conditions of action potential blockade (TTX, ice-cold media) or mimicked without the surgical procedure through optogenetic inhibition of CA3 pyramidal neurons.

Possible explanations for the speed of compensation

Amongst all of the reports of compensatory synaptic responses to chronic alterations in input activity, this response to CA3 removal is relatively rapid. Fast homeostatic plasticity (occurring within four hours of treatment onset) was observed in cultured hippocampal neurons and required both inhibition of action potential discharge and blockade of miniature NMDA receptor currents for induction and was supported by local protein synthesis (Sutton et al., 2006). Similarly, three hours of blockade of AMPARs or NMDARs increased GluA1 at postsynaptic sites (Jakawich et al., 2010). The negative results obtained from the PPF and 30-pulse burst experiments support no change in presynaptic function, suggesting there was no reduction in the frequency of miniature NMDA receptor currents after CA3 resection due to a decrease in transmitter release probability. However, transient presynaptic changes may have occurred during the two-hour incubation period (a brief increase in discharge upon slicing followed by a more persistent depolarization-dependent inactivation). Also, the presynaptic indices that were applied would not be altered by a reduction in the total number of functional afferents, if release parameters remained unaltered at the remaining functional afferents. So, it is possible that, after the immediate response to CA3 removal, because there were fewer functional axons and thus fewer action potentials, there were also fewer transmitter release events and fewer NMDA receptor currents, which might have sped up the homeostatic response (Sutton et al., 2006). A similar procedure to transect Schaffer collaterals *in vivo* also increased excitability at the neuronal population level in area CA1, but the process was reported to be orders of magnitude slower (Dinocourt et al, 2011) and the increased excitability was only observed upon treatment with pro-convulsive chemicals. Unfortunately, the extracellular field recordings were collected no earlier than 24 hours after transection and were taken from the stratum pyramidale only, negating the ability to observe any changes in the Schaffer collateral FV and clouding any measurement of the fEPSP, which was not analyzed. So, it is possible that the same fast homeostatic phenomenon that we observed in the hippocampal slice also occurs *in vivo*.

Another possible explanation for the rapidity of homeostatic adjustment might relate to chemical factors that are released as a result of tissue slicing. It is possible that preparing slices, which severs excitatory neurons, inhibitory neurons, and glia cells, primes widespread plasticity mechanisms and facilitates engagement of these mechanisms following CA3 resection. For example, global scaling up of excitatory synaptic currents due to chronic TTX

Author Manuscript Author Manuscript Author Manuscript Author Manuscript

exposure was shown to be reliant on tumor necrosis factor alpha release from glial cells (TNFα) (Stellwagen and Malenka, 2006). Alternatively, numerous growth factors are released by neurons and glial cells after acute brain injury, including brain derived neurotrophic factor (BDNF), nerve growth factor (NGF), neurotrophin-3 (NT-3) and NT-4 (Meirelles et al., 2017). These growth factors act individually through specific tyrosine receptor kinases (Trks) and all of these factors bind to the P75 receptor. The balance of Trk to P75 activation determines if the neuron will attempt to survive or die after acute injury. Thus, in the hippocampal slice, it may be the case that Trks are selectively activated at the time of preparation, which facilitates growth-related plasticity at the SC-CA1 synapses. In support of this notion, exogenous BDNF delivery can overcome the effects of chronic TTX exposure and blockade of endogenous BDNF mimics the effects of TTX in cortical cultures (Rutherford et al., 1998). The lack of an effect at TA-CA1 synapses might reflect spatial restriction or no involvement of diffusible factors.

Possible explanations for the lack of a presynaptic response to CA3 removal

The increase in presynaptic function observed after global suppression of activity in hippocampal cultures (Bacci et al., 2001; Burrone et al., 2002; Thiagarajan et al., 2002) is absent in the current model. There are numerous potential explanations. First, it may simply be that postsynaptic adjustments can occur acutely, but presynaptic changes require more time. This “postsynaptic before presynaptic” homeostatic plasticity has been demonstrated prior in hippocampal neuronal cultures (Lindskog et al., 2010; Vitureira et al., 2012). Second, it might be the case that presynaptic changes require gene expression and cell bodies. In fact, presynaptic homeostatic plasticity in cultured hippocampal neurons due to activity blockade requires gene expression, while the postsynaptic changes do not (Han and Stevens, 2009). Third, it is possible that presynaptic alterations do occur but are transient or are not apparent with the methods employed. However, a change in the number of functional axons was resolved and numerous assays of presynaptic function that assess different transmitter release properties returned negative results, minimizing the likelihood of a change in presynaptic function. Finally, presynaptic homeostatic plasticity due to global inactivity in hippocampal cultures requires BDNF released from the postsynaptic neuron (Jakawich et al., 2010). The fact that CA3 removal was a presynaptic manipulation may explain the lack of presynaptic homeostatic plasticity.

Synapse-specificity

The compensatory plasticity observed after removal of area CA3 was limited to SC-CA1 synapses and thus is likely not a cell autonomous process that would affect all synapses on CA1 pyramidal neurons, as observed in neuronal cultures during treatment with TTX or bicuculline (Turrigiano et al., 1998; O’Brien et al., 1998). Instead, the plasticity produced by removal of area CA3 is more akin to the synapse-specific homeostatic plasticity produced by removal of the entorhinal cortex from organotypic hippocampal slices (Vlachos et al., 2012) or presynaptic expression of inward-rectifying potassium channels (Hou et al., 2008). Jakawich et al (2012) showed that tonic blockade of AMPARs and NMDARs resulted in increased levels of GluA1, but not GluA2, at the synapses. A similar process may occur in the hippocampal slice preparation following CA3 removal, resulting in insertion of GluA1 homomeric AMPARs at SC-CA1 synapses. Thus, an increase in GluA1 signal in the present

Author Manuscript Author Manuscript Author Manuscript Author Manuscript

report could be due to more GluA1/GluA2 AMPARs at individual synapses, replacement of GluA1/GluA2 AMPARs by GluA1/GluA1 AMPARs, or an increase in the number of AMPAR-containing synapses (Kirov et al., 2004). This issue may be further resolved through Western blot quantification of AMPAR subunits in synaptic fractions, quantification of dendritic spines, which are known to be affected by hippocampal slice preparation (Fiala et al., 2003), and determination of the involvement of specific transmembrane AMPAR regulatory proteins (TARPs) that are known to differentially regulate trafficking of AMPARs with and without GluA2 (Bats et al., 2013). Note, that changes in AMPAR conductance properties or changes in AMPAR insertion at excitatory synapses onto interneurons cannot be ruled out at present.

Summary

Overall, the current study reveals a fast-acting, synapse-specific compensatory increase in synaptic efficacy in the hippocampal slice preparation lacking area CA3. While this slice preparation is relatively common, this homeostatic phenomenon has likely not been reported because laboratories have not directly compared between slices with and without area CA3 intact. Unlike slower forms of homeostatic plasticity, this newly discovered rapid compensatory response exhibits the temporal dynamics that might allow it to keep pace with high levels of ongoing activity-dependent plasticity in the hippocampus *in vivo* (Toyoizumi et al., 2014; Jedlicka et al., 2015 Zenke et al., 2017). A better understanding of this phenomenon may offer a new perspective on recovery from traumatic brain injury and present new therapeutic targets.

Acknowledgments

This research was supported by the Krasnow Institute for Advance Study at George Mason University, the National Institutes of Health (NIA, R15AG045820-01A1) and the Department of Defense (ONR#000141010198). All authors declare no conflict of interest.

References

Aptowicz CO, Kunkler PE, Kraig RP. Homeostatic plasticity in hippocampal slice cultures involves changes in voltage-gated Na+ channel expression. Brain Res. 2004; 998(2):155–63. [PubMed: 14751586]

Bacci A, Coco S, Pravettoni E, Schenk U, Armano S, Frassoni C, Verderio C, De Camilli P, Matteoli M. Chronic blockade of glutamate receptors enhances presynaptic release and downregulates the interaction between synaptophysin-synaptobrevin-vesicle-associated membrane protein 2. J Neurosci. 2001; 21(17):6588–96. [PubMed: 11517248]

Bats C, Farrant M, Cull-Candy SG. A role of TARPs in the expression and plasticity of calcium-permeable AMPARs: evidence from cerebellar neurons and glia. Neuropharmacology. 2013 Nov. 74:76–85. [PubMed: 23583927]

Burrone J, O'Byrne M, Murthy VN. Multiple forms of synaptic plasticity triggered by selective suppression of activity in individual neurons. Nature. 2002; 420(6914):414–8. [PubMed: 12459783]

Dailey ME, Buchanan J, Bergles DE, Smith SJ. Mossy fiber growth and synaptogenesis in rat hippocampal slices in vitro. J Neurosci. 1994; 14(3 Pt 1):1060–78. [PubMed: 8120613]

Dinocourt C, Aungst S, Yang K, Thompson SM. Homeostatic increase in excitability in area CA1 after Schaffer collateral transection invivo. Epilepsia. 2011; 52(9):1656–65. [PubMed: 21635239]

Félix-Oliveira A, Dias RB, Colino-Oliveira M, Rombo DM, Sebastião AM. Homeostatic plasticity induced by brief activity deprivation enhances long-term potentiation in the mature rat hippocampus. J Neurophysiol. 2014; 112(11):3012–22. [PubMed: 25210161]

Author Manuscript Author Manuscript Author Manuscript Author Manuscript

Fiala JC, Kirov SA, Feinberg MD, Petrak LJ, George P, Goddard CA, Harris KM. Timing of neuronal and glial ultrastructure disruption during brain slice preparation and recovery in vitro. J Comp Neurol. 2003; 465(1):90–103. [PubMed: 12926018]

Galvan CD, Wenzel JH, Dineley KT, Lam TT, Schwartzkroin PA, Sweatt JD, Swann JW. Postsynaptic contributions to hippocampal network hyperexcitability induced by chronic activity blockade in vivo. Eur J Neurosci. 2003; 18(7):1861–72. [PubMed: 14622219]

Han EB, Stevens CF. Development regulates a switch between post- and presynaptic strengthening in response to activity deprivation. Proc Natl Acad Sci USA. 2009; 106(26):10817–22. [PubMed: 19509338]

Hou Q, Zhang D, Jarzylo L, Huganir RL, Man HY. Homeostatic regulation of AMPA receptor expression at single hippocampal synapses. Proc Natl Acad Sci USA. 2008; 105(2):775–80. [PubMed: 18174334]

Ibata K, Sun Q, Turrigiano GG. Rapid synaptic scaling induced by changes in postsynaptic firing. Neuron. 2008; 57(6):819–26. [PubMed: 18367083]

Jakawich SK, Nasser HB, Strong MJ, McCartney AJ, Perez AS, Rakesh N, Carruthers CJ, Sutton MA. Local presynaptic activity gates homeostatic changes in presynaptic function driven by dendritic BDNF synthesis. Neuron. 2010; 68(6):1143–58. [PubMed: 21172615]

Jedlicka P, Benuskova L, Abraham WC. A Voltage-Based STDP Rule Combined with Fast BCM-Like Metaplasticity Accounts for LTP and Concurrent “Heterosynaptic” LTD in the Dentate Gyrus In Vivo. PLoS Comput Biol. 2015; 11(11):e1004588. [PubMed: 26544038]

Ju W, Morishita W, Tsui J, Gaietta G, Deerinck TJ, Adams SR, Garner CC, Tsien RY, Ellisman MH, Malenka RC. Activity-dependent regulation of dendritic synthesis and trafficking of AMPA receptors. Nat Neurosci. 2004; 7(3):244–53. [PubMed: 14770185]

Kim J, Tsien RW. Synapse-specific adaptations to inactivity in hippocampal circuits achieve homeostatic gain control while dampening network reverberation. Neuron. 2008; 58(6):925–37. [PubMed: 18579082]

Kirov SA, Petrak LJ, Fiala JC, Harris KM. Dendritic spines disappear with chilling but proliferate excessively upon rewarming of mature hippocampus. 2004; 127(1):69–80.

Lindskog M, Li L, Groth RD, Poburko D, Thiagarajan TC, Han X, Tsien RW. Postsynaptic GluA1 enables acute retrograde enhancement of presynaptic function to coordinate adaptation to synaptic inactivity. Proc Natl Acad Sci USA. 107:806–811.

da Silva Meirelles L, Simon D, Regner A. Neurotrauma: The Crosstalk between Neurotrophins and Inflammation in the Acutely Injured Brain. Int J Mol Sci. 2017; 18(5) pii: E1082.

Mockett BG, Hulme SR. Metaplasticity: new insights through electrophysiological investigations. J Integr Neurosci. 2008; 7:315–36. [PubMed: 18763726]

Nguyen PV, Kandel ER. A macromolecular synthesis-dependent late phase of long-term potentiation requiring cAMP in the medial perforant pathway of rat hippocampal slices. J Neurosci. 1996; 16(10):3189–98. [PubMed: 8627357]

O’Brien RJ, Kamboj S, Ehlers MD, Rosen KR, Fischbach GD, Huganir RL. Activity-dependent modulation of synaptic AMPA receptor accumulation. Neuron. 1998; 21(5):1067–78. [PubMed: 9856462]

Rich MM, Wenner P. Sensing and expressing homeostatic synaptic plasticity. Trends Neurosci. 2007; 30(3):119–25. [PubMed: 17267052]

Royer S, Paré D. Conservation of total synaptic weight through balanced synaptic depression and potentiation. Nature. 2003; 422(6931):518–22. [PubMed: 12673250]

Rutherford LC, Nelson SB, Turrigiano GG. BDNF has opposite effects on the quantal amplitude of pyramidal neuron and interneuron excitatory synapses. Neuron. 1998; 21(3):521–30. [PubMed: 9768839]

Stellwagen D, Malenka RC. Synaptic scaling mediated by glial TNF-alpha. Nature. 2006; 440(7087): 1054–9. [PubMed: 16547515]

Sutton MA, Ito HT, Cressy P, Kempf C, Woo JC, Schuman EM. Miniature neurotransmission stabilizes synaptic function via tonic suppression of local dendritic protein synthesis. Cell. 2006; 125(4): 785–99. [PubMed: 16713568]

Author Manuscript Author Manuscript Author Manuscript Author Manuscript

Thiagarajan TC, Piedras-Renteria ES, Tsien RW. alpha- and betaCaMKII. Inverse regulation by neuronal activity and opposing effects on synaptic strength. Neuron. 2002; 36(6):1103–14. [PubMed: 12495625]

Toyoizumi T, Kaneko M, Stryker MP, Miller KD. Modeling the dynamic interaction of Hebbian and homeostatic plasticity. Neuron. 2014; 84(2):497–510. [PubMed: 25374364]

Turrigiano GG, Leslie KR, Desai NS, Rutherford LC, Nelson SB. Activity-dependent scaling of quantal amplitude in neocortical neurons. Nature. 1998; 391(6670):892–6. [PubMed: 9495341]

Turrigiano GG, Nelson SB. Homeostatic plasticity in the developing nervous system. Nat Rev Neurosci. 2004; 5:97–107. [PubMed: 14735113]

Tyler WJ, Pozzo-Miller L. Miniature synaptic transmission and BDNF modulate dendritic spine growth and form in rat CA1 neurones. J Physiol. 2003; 553(Pt 2):497–509. [PubMed: 14500767]

Vitureira N, Letellier M, Goda Y. Homeostatic synaptic plasticity: from single synapses to neural circuits. Curr Opin Neurobiol. 2012; 22(3):516–21. [PubMed: 21983330]

Vlachos A, Becker D, Jedlicka P, Winkels R, Roeper J, Deller T. Entorhinal denervation induces homeostatic synaptic scaling of excitatory postsynapses of dentate granule cells in mouse organotypic slice cultures. PLoS One. 2012; 7(3):e32883. [PubMed: 22403720]

Zenke F, Gerstner W, Ganguli S. The temporal paradox of Hebbian learning and homeostatic plasticity. Curr Opin Neurobiol. 2017; 43:166–176. [PubMed: 28431369]

Author Manuscript Author Manuscript Author Manuscript Author Manuscript

Highlights

- Area CA3 is commonly removed from acutely prepared hippocampal slices
- CA3 removal reduces the Schaffer collateral input to area CA1 pyramidal neurons
- CA3 removal increases efficacy of Schaffer collateral synapses
- The synaptic response to CA3 removal normalizes pyramidal cell discharge in area CA1

Author Manuscript Author Manuscript Author Manuscript Author Manuscript

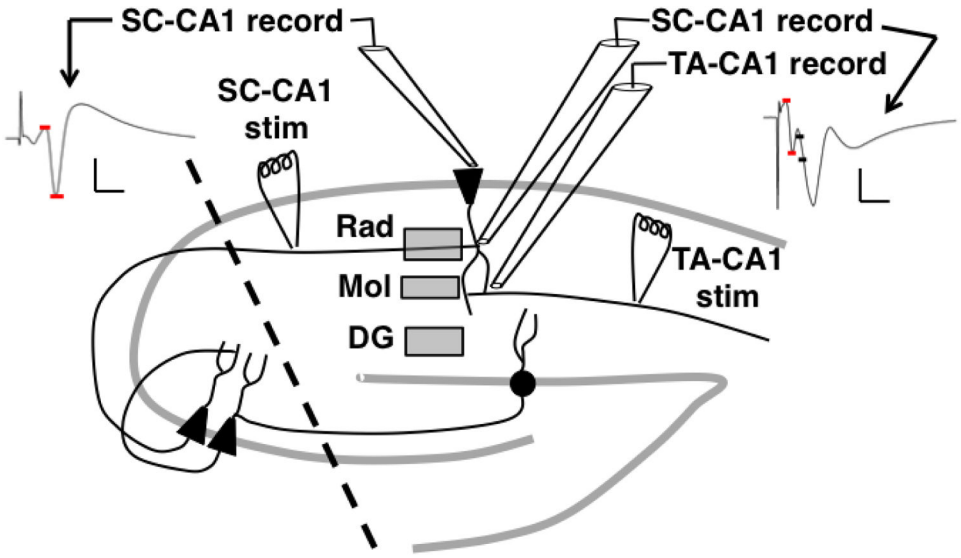

Figure 1.

Drawing of the hippocampal slice preparation depicting the cut site to remove area CA3 and electrode positions for recording of SC-CA1 and TA-CA1 synaptic responses. The CA3 removal cut is represented by a thick dashed line. Stimulating and recording electrode positions to elicit and record SC-CA1 and TA-CA1 synaptic responses are shown and labeled accordingly. Note that SC-CA1 responses are measured in stratum radiatum and stratum pyramidale simultaneously. Boxes denote GluA1 signal extraction regions. Stratum radiatum, RAD; stratum molecular, MOL; dentate gyrus, DG. Waveforms are example traces recorded in the stratum pyramidale (left) and stratum radiatum (right). Red cursors are placed to extract the PS and FV amplitudes. Black cursors denote extraction region for the fEPSP slope.

Author Manuscript Author Manuscript Author Manuscript Author Manuscript

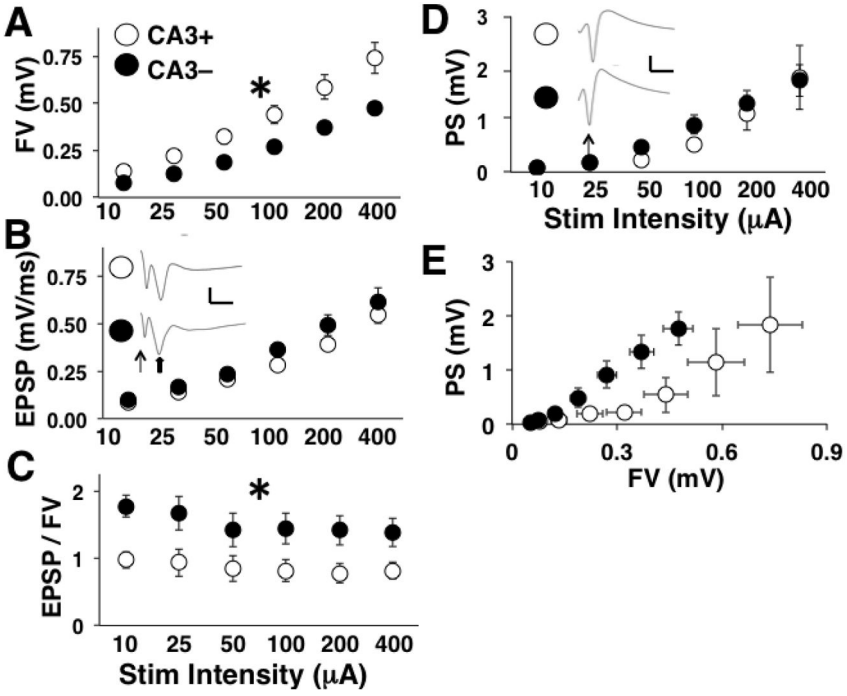

Figure 2.

Schaffer collateral I/O curve results. For all panels, CA3+ denotes the slices with CA3 intact and CA3- denotes the slices with CA3 removed. **A)** Mean FV amplitude at each stimulation level. Mean values are based on 16 slices (7 animals) for CA3+ and 17 slices (7 animals) for CA3-. **B)** Mean fEPSP slope at each stimulation level. Insets show averaged waveforms of all sweeps at the highest stimulation level for CA3+ and CA3- slices. Scale bars are 1 mV and 10 ms. Line arrow points to the FV. Block arrow points to the fEPSP. **C)** Mean fEPSP to FV ratios at each stimulation level. **D)** Mean PS amplitude at each stimulation level. * indicate a significant main effect of CA3 removal at $p < 0.05$. Insets show averaged waveforms of all sweeps at the highest stimulation level for CA3+ and CA3- slices. Scale bars are 1 mV and 10 ms. Line arrow points to the FV.

Author Manuscript Author Manuscript Author Manuscript Author Manuscript

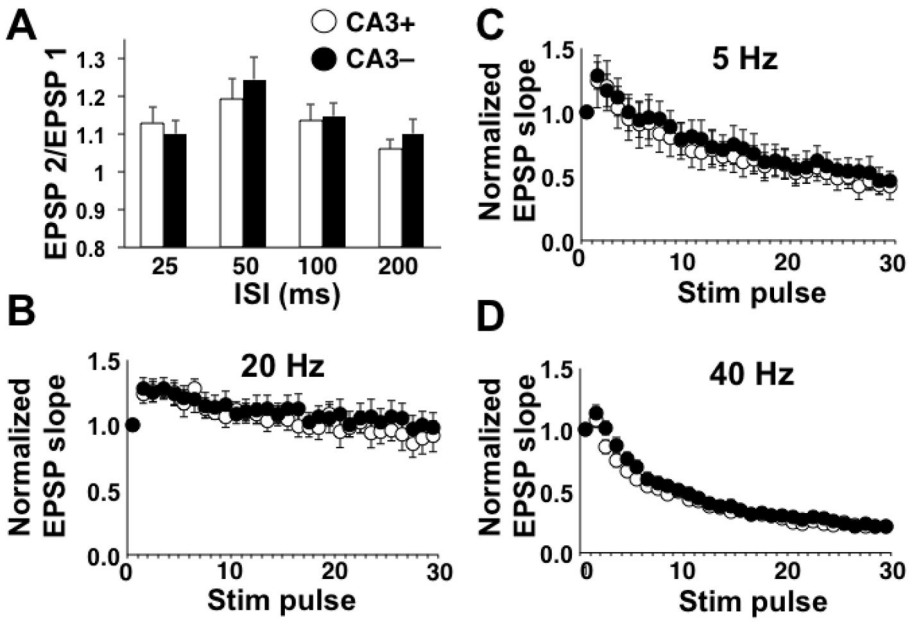

Figure 3.

PPF and high frequency burst results. For all panels, CA3+ denotes the slices with CA3 intact and CA3- denotes the slices with CA3 removed. **A)** Mean PPF values at each ISI. Mean values are based on 20 slices (6 animals) for the CA3+ group and 19 slices (6 animals) for the CA3- group. **B)** Mean normalized fEPSP slope for each stimulation pulse delivered at 5 Hz. Mean values are based on 7 slices (4 animals) for CA3+ and 8 slices (4 animals) for CA3-. **C)** Mean normalized fEPSP slope for each stimulation pulse delivered at 20 Hz. Mean values are based on 8 slices (4 animals) for CA3+ and 8 slices (4 animals) for CA3-. **D)** Mean normalized fEPSP slope for each stimulation pulse delivered at 40 Hz. Mean values are based on 17 slices (10 animals) for CA3+ and 13 slices (9 animals) for CA3-.

Author Manuscript Author Manuscript Author Manuscript Author Manuscript

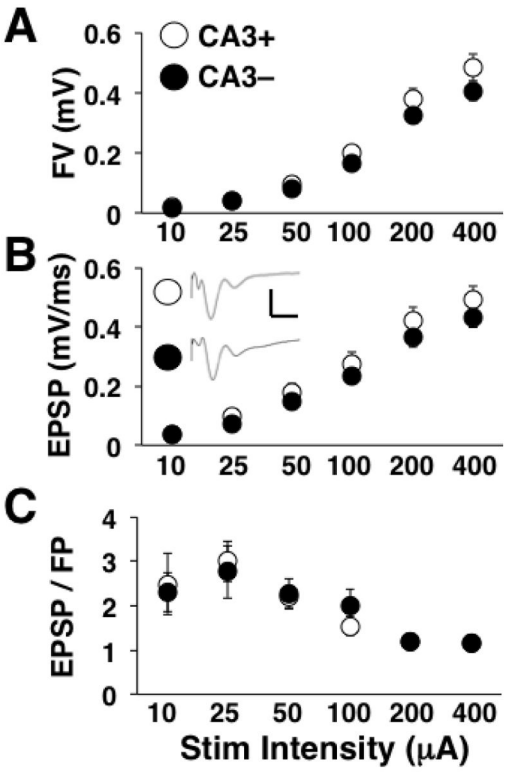

Figure 4.

TA-CA1 I/O curve results. For all panels, CA3+ denotes the slices with CA3 intact and CA3- denotes the slices with CA3 removed. **A)** Mean FV amplitude at each stimulation level. **B)** Mean fEPSP slope at each stimulation level. Insets show averaged waveforms of all sweeps at the highest stimulation level for CA3+ and CA3- slices. Scale bars are 1 mV and 10 ms. **C)** Mean fEPSP to FV ratios at each stimulation level. Mean values are based on 19 slices (5 animals) for CA3+ and 19 slices (5 animals) for CA3-.

Author Manuscript Author Manuscript Author Manuscript Author Manuscript

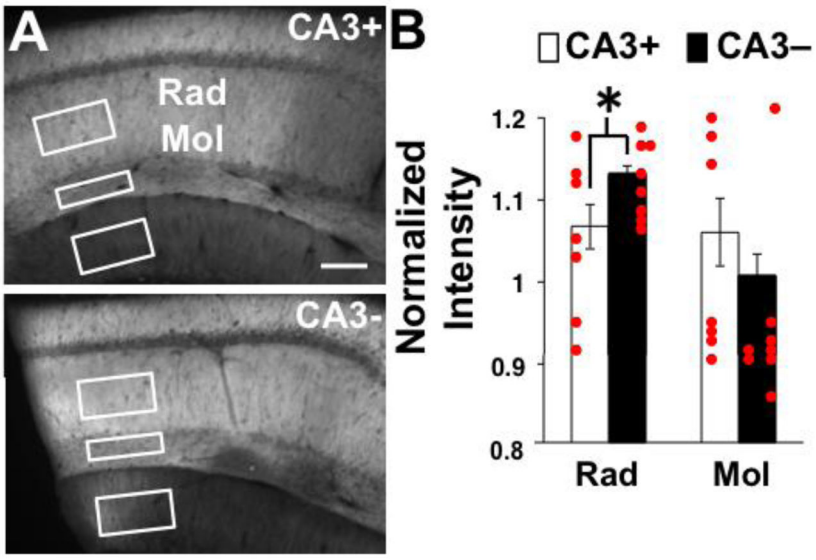

Figure 5.

GluR1 IHC results. **A)** Images of labeled slices. CA3+ denotes the slice with CA3 intact and CA3- denotes the slice with CA3 removed. Boxes illustrate regions for extraction of mean signal intensity. Scale bar is 100 μm. **B)** Quantification of normalized mean signal intensities measured in stratum radiatum and stratum moleculare. Mean values are based on 7 animals for CA3+ and 8 animals for CA3-. * indicates a significant difference between groups at $p < 0.05$.